Shear Assessment of Precast composite girders using FprEN 1992-1 based shear expressions

Mohammed S. Ibrahim[1], Marco Roosen[1,2] , Max A.N. Hendriks[1,3] and Yuguang Yang[1]

[1]Faculty of Civil Engineering and Geosciences,
Delft University of Technology,
the Netherlands,

[2]Rijkswaterstaat, Ministry of Infrastructure and Water Management,
the Netherlands

[3]Department of Structural Engineering,
Norwegian University of Science and Technology (NTNU),
Norway,

M.S.Ibrahim-1@tudelft.nl

Abstract

Inverted T precast girders with a cast-in-situ topping layer, recognized as precast composite girders, are commonly used in Dutch bridge construction. Notably, the bridges built before 1974 often lacked sufficient shear reinforcement, raising concerns about their shear capacity under increasing traffic loads. However, how to assess these composite girders under the scope of the second-generation Eurocode remains challenging, as the shear formulations were originally developed for monolithic structural members. Consequently, their direct applicability to precast composite systems, due to the distinctive stress distribution in the web of the composite structural members, lacks theoretical substantiation and experimental validation. This study first presents the three alternative failure criteria equations based on the same theory, and after that, an experimental investigation of the shear behaviour of precast composite girders through two full-scale tests is discussed. The test data is later used to compare the alternative failure criteria.

1 Introduction

Inverted T precast girders with cast-in-situ topping layer, hereafter referred to as Precast composite girders, are widely used for bridge construction in the Netherlands. Many of these post-WWII constructed bridges are reaching their initial design life and require a reassessment of their capacity to accommodate the increased traffic loading. Notably, the bridges built before the introduction of minimum shear reinforcement in 1974 lack sufficient shear reinforcement and pose significant concerns regarding their shear capacity.

Shear failure occurs suddenly and with little warning, making accurate assessment methods crucial for evaluating existing structures. However, assessing composite members remains challenging, as current shear formulations, including the upcoming second-generation Eurocode [1], were originally developed for monolithic structural members. Consequently, their direct applicability to precast composite systems, due to the distinctive stress distribution in the web of the composite structural members, lacks theoretical substantiation and experimental validation. In this context, the second-generation Eurocode emerges as a candidate for the shear assessment of precast composite members, as it is recognised as a model that is more linked to physical parameters. For that reason, the Dutch Ministry of Infrastructure and Water Management is considering to introduce a formulation based on the second-generation Eurocode to evaluate the precast composite girders in the Netherlands. To that end, this study first presents a set of different shear expressions that are based on the general concept presented in FprEN 1992-1-1 and can be considered as a candidate for the assessment of the precast composite

girders. The various expressions are further assessed using two recently conducted full-scale experimental observations on the shear behaviour of precast composite girders.

2 Implementation of CSCT based shear formulas for precast composite girders

The shear formulation for members without shear reinforcement in the second generation of Eurocode is based on the critical shear crack theory (CSCT) [2].The theory links the resistance of a structural member to the average strain of a critical shear crack through a failure criterion given as a simplified expression. From its inception to the final current code format simplification, multiple failure criteria can be recognized from literature. The following section briefly reviews the different forms.

The original form of CSCT proposed by Muttoni and Fernández Ruiz [2] is given in Equation 1. According to the original formula, the term εd represents the product of the average strain at mid-depth of the structural member and the average crack spacing at mid-depth. This represents the width of the critical shear crack. Equation 1 is modified for code application in FprEN 1992- 1-1:2023 [1] Annex I.8. The term ε is replaced by ε_v in Equation 2 (Equation I.7 in FprEN 1992- 1-1:2023), which represents the strain of longitudinal reinforcement instead of the original definition, in addition partial safety factors, including the uncertainty of determining strain deformation is included in the equation. This equation is mainly to be used for assessing existing structures. To facilitate the ease of application in designing new structures, the failure criteria is further modified in a power-law form (Equation 8.27 in FprEN 1992- 1-1:2023). In the equation, the influence of the inclination of the critical shear crack is considered by a coefficient (k) [3] . Fig. 1 summarises the above-presented failure criterias.

$$\frac{V_R}{bd\sqrt{f_c}} = \frac{1}{6}\frac{2}{1+120\dfrac{\varepsilon d}{16+d_g}} \tag{1}$$

where :

ε at $0.6d$ from the compression face

$$\tau_{Rd,c} = 0.33\frac{\gamma_{def}^{2/3}}{\gamma_v}\frac{\sqrt{f_{ck}}}{1+24\gamma_{def}\,\varepsilon_v\dfrac{d}{d_{dg}}} \tag{2}$$

where :

ε_v is the strain at the longitudinal rebar

$$V_{Rc} = k\left(\frac{f_c\, d_{dg}}{\varepsilon_v\, d}\right)^{\frac{1}{2}} b_w\, d \tag{3}$$

where : $k = 0.015\left(\dfrac{a_{cs}}{d}\right)^{\frac{1}{4}}$

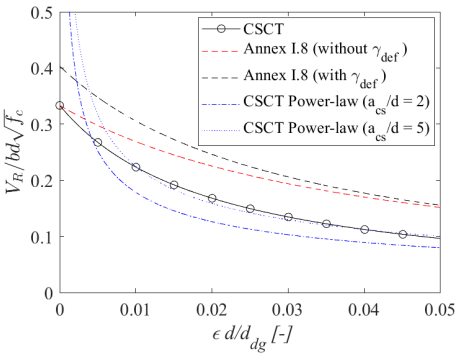

Fig. 1 CSCT failure criterions

For consistent observation, Fig. 1 is prepared by using the strain at tension reinforcement level and the relation $\varepsilon = 0.41\ \varepsilon_v$ for the original CSCT (see Equations 1 and 2). As can be seen from the plot, the CSCT power law gives a lower bound estimate for the selected shear slenderness. It is also interesting to note that Annex I.8 is not identical to the original models and provides a higher capacity estimate throughout the range. Recently, a comprehensive validation of the different forms of CSCT for monolithic prestressed concrete girders was conducted [4]. The validation indicates that the FprEN 1992-1-1:2023 shear formula (derived based on the power-law failure criterion) showed conservative results in all test specimens. However, Equation 2, the failure criterion of Annex I.8, is observed to overestimate the shear resistance of specimens with a_{cs}/d larger than 3.

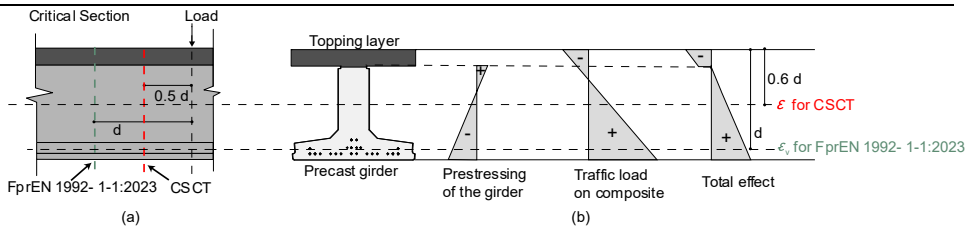

Fig. 2 Strain distribution of precast continuous members (a) Critical sections (b) Strain distribution and reference strain for the failure criteria

As discussed, the three failure criteria were originally proposed for monolithic members. Furthermore, the power-law failure criterion is simplified to Equation 8.27 in FprEN 1992- 1-1:2023, considering a linear elastic behaviour and strain distribution. The precast composite girders exhibit different strain distributions at failure than those expected on monolithic elements. A typical strain distribution of such a structure is given in Fig. 2. As shown in the figure, the total strain distribution of the composite members is composed of the prestressing effect on the precast girder and the traffic load effect on the composite element. This distinct strain distribution makes the direct application of the standard shear formula of the FprEN 1992-1-1:2023(Equation 8.27) unviable. Given the absence of validation on similar elements and an urgent need for assessment, we present an initial comparison of the selected general failure criterions with recently conducted full-scale experiments.

3 Experimental Specimens

This section presents the details of two specimens that form part of a larger group to study the shear behaviour of continuous precast girders. In the test program, 15 m-long continuous specimens are designed and tested in two phases. In testing phase 1, as shown in Fig. 3, the specimens are externally clamped in the end support region and loaded in the main span and cantilever end. This results in failure close to the intermediate region [5]. In testing phase 2, the damaged end is repaired, and the girders are loaded only in the main span as a simply supported specimen. The presented tests are performed in testing phase 2.

Both specimens, S12HLC_S and S06SSC, are made of Inverted T precast girders with a depth of 900 mm and a cast in-situ topping layer of 160 mm. Specimen S12HLC_S is a girder without shear reinforcement tested with a shear slenderness of 4.4 in the manner described (see Fig. 3).

Specimen S06SSC is designed and tested for a slenderness of 6.4. The specimen was provided with shear reinforcement with a diameter of 6 mm spaced at 240 mm. The provided reinforcement is below the minimum requirement of Eurocode, and the girder can be considered a member without shear reinforcement. Due to its larger tested shear span, a 15 m-long girder was cast and tested without prior testing.

3.1 Material properties

The precast beams are cast using a self-compacting concrete mix with a maximum aggregate size of 16 mm. The topping layer was cast using normal-strength concrete with a similar aggregate size. Table 1 presents the average cubic strength of the concrete for the precast girder and topping layer.

Table 1 Summary of the test specimens

Specimen	ρ_w, [%]	σ_{cp} † [MPa]	a/d	Concrete	
				Girder $f_{c,cube}$ [MPa]	Topping $f_{c,cube}$ [MPa]
S12HLC_S	-	3.52	4.4	95.7	71.4
S06SSC	0.078	3.52	6.4	98.5	72.6

- *† Central prestress for the precast girder, considering losses*
- *Age of girder at testing: S12HLC_S - 407 days, S06SSC- 415 days ,*

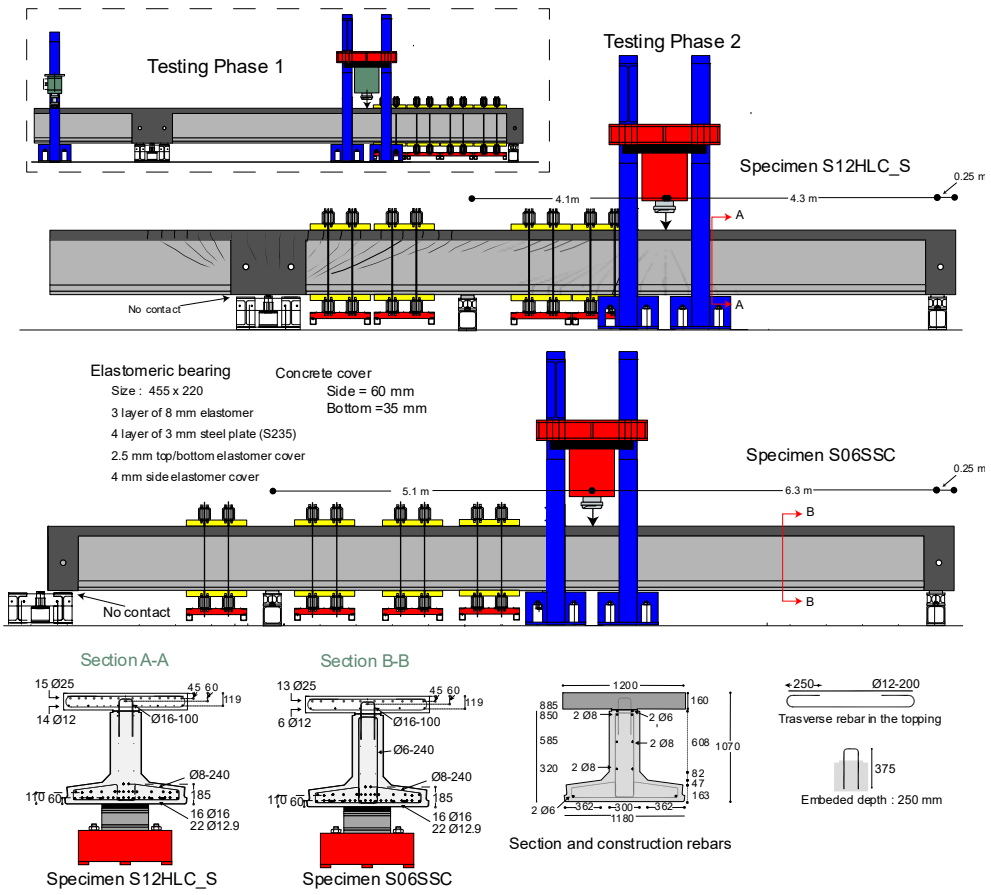

Fig. 3 Details of the specimens (all dimensions are in mm)

The precast beams are prestressed with twenty-two 7-wire prestressing strands (FeP 1860) with a diameter of 12.9 mm. For both specimens, each strand was initially pretensioned to 79 kN. This translates into a central prestress of 4 MPa before loss. The introduction of prestress to the concrete during release and prestress losses until testing were monitored using embedded fibre optic sensors. The measurement indicated the total prestress loss on the day of testing was 12 per cent for both specimens. Steel rebars with a specified grade of B500B are used for the longitudinal and shear reinforcement.

3.2 Test setup, loading protocol and sensor plan

Fig. 3 shows the boundary conditions of the experiment. The specimens are supported at both ends using elastomeric bridge bearings. A hydraulic jack with a capacity of 5 MN is used to apply the load on the specimens. Steel loading plates with 300 × 300 × 20 mm dimensions introduce the force to the specimen. In both tests, the loading was applied in displacement control loading with a constant loading rate of 0.02 mm/s. The sensor plan of the test included monitoring average displacement using LVDT grids and detailed cracking evolution using Digital Image Correlation (DIC). Due to space constraints, only selected crack patterns using the DIC principal strain and the test global response are presented here.

4 Experimental observation

Both specimens failed in shear in the interest zone. Fig. 4 and Fig. 5 show the shear force-displacement response of the specimens S12HLC_S and S06SSC. Along with the global response, the cracking state at selected stages is presented, accompanied by a brief explanation of the failure process.

Specimen S12HLC_S is a member without shear reinforcement and was tested for shear slenderness of 4.4. The load-displacement response of the specimen initially showed a linear response followed by softened post-cracking stiffness. The change in the stiffness is observed due to the opening of multiple flexural shear cracks from the previous testing phase at the shear force of 382 kN. Additional loading results in the propagation of flexural shear cracks (see cracking state at shear force of 676 kN). Further increases in the applied loading initiated secondary cracks below the hairpin (interface) reinforcement, leading to the failure of beam action (marked by a diamond in the shear force-displacement plot). This shift in resistance mechanism can be observed from the Shear force-deflection response, showing a significant change in post-crack stiffness. Beyond this point, additional loading primarily caused more shear cracking, and the arching action contributed to further load resistance. The specimen reached its peak capacity at 851 kN, and failure resulted due to web crushing above the exterior shear crack. Fig. 4 shows the post-peak state of the specimen.

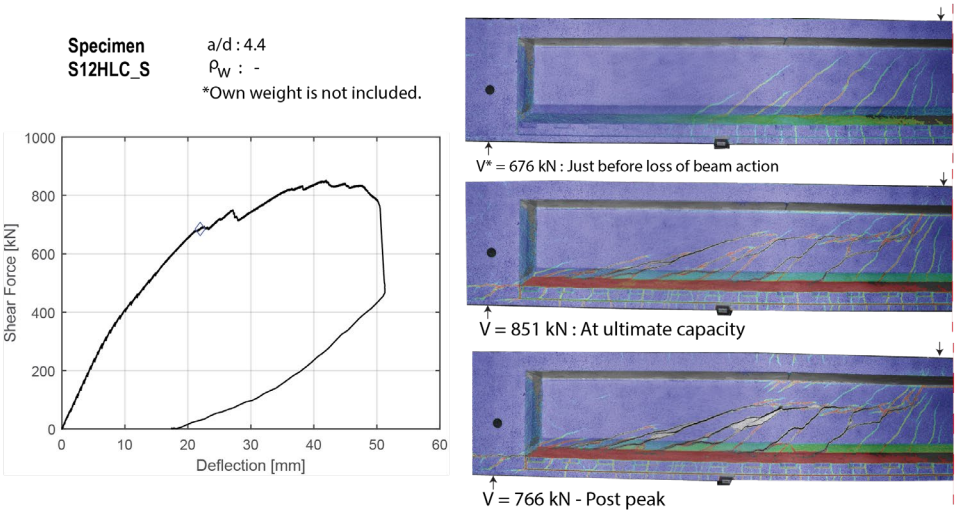

Fig. 4 Experimental result of S12HLC_S (a) Shear force-deflection (left) (b) Cracking state at selected stages (right)

Specimen S06SSC is tested for a shear slenderness of 6.4. The global response of specimen S06SSC showed a linear response followed by softened post-cracking stiffness. The first cracking is observed under the loading region at a shear force of 286 kN. Further loading results in the initiation and propagation of several flexural shear cracks. The cracking state at the shear force of 519 kN is shown in Fig. 5. An additional increase in loading causes the merging of the shear crack below the hairpin reinforcement. The beam action is lost at this stage, and the arching mechanism resists further loading. The transition to the arching mechanism is indicated in the global response (see the diamond indication). Unlike Specimen S12HLC_S, a noticeable shift in the global post-crack stiffness was not observed. The specimen reached its peak capacity at a total shear force of 591 kN, and its cracking state is shown in Fig. 5. Further loading results in the initiation of additional shear cracks, which results in a small load drop and further softens the response to a seemingly ductile response. The specimens ultimately failed due to the web failure from reinforcement rupture, resulting in a load drop of 12 per cent.

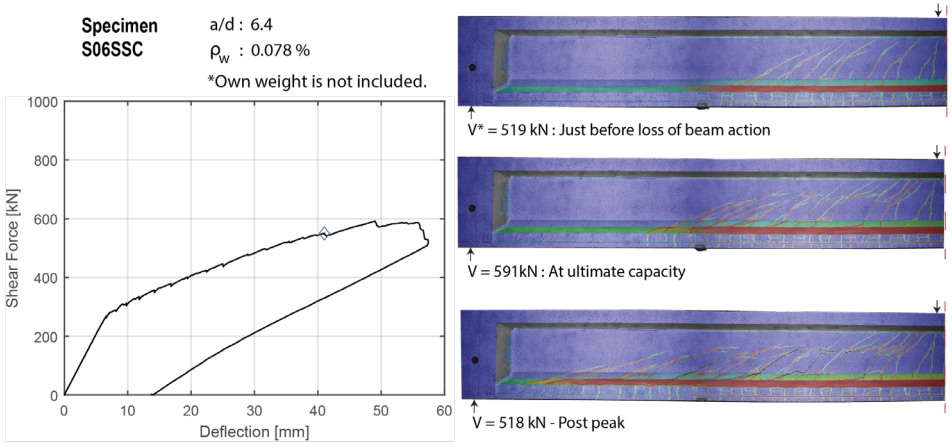

Fig. 5 Experimental result of S06SSC (a) Shear force-deflection (left) (b) Cracking state at selected stages (right)

Despite the specimen being tested with a/d ratio of 6.4, arching action was still able to sustain the load after the failure of the beam action. This contrasts with the common assumption that the arching mechanism becomes less effective for shear slenderness ratios greater than 2.5, as observed in reinforced concrete members. One possible explanation for this behaviour is the influence of local interface reinforcement. In both tests, flexural shear cracks merged beneath the interface reinforcement. The relatively higher amount of interface reinforcement may have created favourable conditions to form a stable arching mechanism, possibly together with other shear-resisting mechanisms. Additional experimental investigations are needed to substantiate this observation. Nevertheless, the findings from these tests on the arching mechanism may provide valuable insights for assessing the capacity of similar existing bridges.

5 Comparison of the tests against the CSCT failure criterions

To determine the shear capacity using the code-based CSCT failure criteria, the strain at the longitudinal tensile reinforcement, ε_v, at a defined critical section must be evaluated. (see Fig. 2). In contrast, the original CSCT model is based on the strain at 0.6d from the extreme compression layer. Considering the distinct strain distribution in the composite members, a nonlinear sectional analysis that accounts for the construction sequence and prestressing forces is conducted to determine the reference strains. By using this nonlinear sectional analysis in an iterative calculation scheme, the shear capacity of the specimens is evaluated according to each failure criterion.

Table 2 presents the experimental shear capacity and prediction of the selected CSCT criterions. For direct comparisons with the test, the shear force due to the weight of the girder at the defined critical section shall be reduced from the prediction.

Table 2 Experimental result and predicted capacities of the selected CSCT criteria

Specimen	ρ_w, [%]	*a/d*	V_{Exp}, kN	V_{FprEN}†, kN	$V_{Annex\ I}$ †, kN	V_{CSCT} †, kN	$V_{Exp}/V_{FprEN,\ Annex.I\ CSCT}$
S12HLC_S	-	4.4	851	538	606	504	1.5,1.34,1.60
S06SSC	0.078	6.4	591	364	457	358	1.6,1.29, 1.65

† *Own weight effect is not reduced.*

At critical location d: Shear force due to own weight for S06SSC ~ 0 kN, S12HLC_S = -23 kN

At critical location 0.5.d : Shear force due to own weight for S06SSC : -9 kN , S12HLC_S = -30 kN

Generally, all of the selected approaches provide safe and conservative predictions. The original CSCT provides the most conservative result, while Annex I delivers the best overall prediction. The power-law prediction falls between the predictions of the other CSCT criteria. Although the selected approaches yield safe predictions, the observed failure modes are inconsistent with the assumed failure mode of the CSCT criteria. Contrary to the aggregate interlock failure assumption of the CSCT [2], the ultimate capacity of both specimens was controlled by the arching capacity.

6 Conclusions

In the context of evaluating the shear resistance of precast composite bridge girders without shear reinforcement, this paper examines three shear equations related to the FprEN 1992-1-1 shear approach for structural concrete members. Considering the lack of validation for similar structural systems, the current study compared different forms of the code equation using insights from recent experiments.

Two full-scale specimens designed to represent existing bridges are tested at shear slenderness of 4.4 and 6.4. Based on the experimental result and comparison, the following conclusions are reached.

- The experiments showed that, even with a shear slenderness of 6.4, the precast composite girders were able to transfer loads through arching action once beam action failed. However, since the failure mechanism of both tests was highly affected by the interface reinforcement, additional experiments will be needed to fully substantiate the observation.
- The comparison between the test results and selected approaches indicates that all the chosen forms of CSCT provide safe estimates for the shear strength of the girders.
- Among the different CSCT formulations, Annex I equation delivers the highest prediction, while the original CSCT offers a lower bound estimate, with the power-law model providing an intermediate prediction.
- Although the CSCT approaches offer safe predictions, the observed failure modes in the tests did not align with those assumed in the model. Models that consistently incorporate the observed failure modes can be valuable for more accurate capacity assessments of similar existing bridges.

Acknowledgements

The authors wish to express their gratitude and sincere appreciation to the Dutch Ministry of Infrastructure and the Environment (Rijkswaterstaat) for financing this research work.

References

[1] CEN/TC 250/SC 2 N 2078., 2023. FINAL DRAFT FprEN 1992-1-1-Eurocode 2-Design of concrete structures-Part 1-1: General rules and rules for buildings, bridges and civil engineering structures.

[2] Muttoni, A., Fernández Ruiz, M., 2008. “Shear Strength of Members without Transverse Reinforcement as Function of Critical Shear Crack Width.” ACI Structural Journal: 163–72.

[3] Miguel, P.F., Fernández, M.A., Hegger, J., Schmidt, M., 2023. “Shear Resistance of Members Without Shear Reinforcement in Presence of Compressive Axial Forces in the Next Eurocode 2.” Hormigon y Acero 74(299–300): 41–60, Doi: 10.33586/hya.2023.3112.

[4] Park, M.K., Yang, Y., Roosen, M., 2024. Validation of CSCT Strain-based Shear Failure Criteria for Prestressed Concrete Members without Shear Reinforcement. 20th fib Symposium on ReConStruct: Resilient Concrete Structures, 2024, fib. The International Federation for Structural Concrete p. 2858–68.

[5] Ibrahim, M.S., Yang, Y., Roosen, M., Hendriks, M.A.N., 2022. Challenges on the shear behavior of existing continuous precast girder bridges. Proc. of the 14th fib International PhD Symposium in Civil Engineering,.